Dopant Substitution and Ion Migration in the $LaGaO_3$-Based Oxygen Ion Conductor

M. S. Khan and M. S. Islam*

Department of Chemistry, University of Surrey, Guildford GU2 5XH, U.K.

D. R. Bates

BG plc, Gas Research and Technology Centre, Ashby Road, Loughborough LE11 3GR, U.K.

Received: October 1, 1997; In Final Form: December 31, 1997

Computer-modeling techniques have been used to investigate the defect and transport properties of the $LaGaO_3$-based oxygen ion conductor. We consider a range of cation dopant substitutions with oxygen vacancy compensation. Favorable acceptor dopants (on energetic grounds) are predicted to be Sr at La and Mg at Ga, in accord with experimental work. The formation of dopant−vacancy clusters is examined with the lowest binding energy found for the Sr−vacancy configuration. Oxygen-vacancy migration is along the GaO_6 octahedron edge with a curved trajectory and a calculated migration energy of 0.73 eV. We have also examined cation-vacancy transport, which reveals high migration energies (>4 eV). Hole formation from an oxidation process is calculated to be relatively unfavorable, which is compatible with experimental findings that show predominantly ionic conduction in doped $LaGaO_3$. Furthermore, consideration of water incorporation suggests that proton conduction will not be significant in this material.

Introduction

The search for oxide materials with high oxygen ion conductivity has attracted much attention owing to both the technological applications (e.g., fuel cells, oxygen separation membranes) and the fundamental interest of high ionic mobility in inorganic solids.[1,2] Fluorite-structured oxides, particularly Y_2O_3-stabilized ZrO_2, are the most common electrolytes used in solid oxide fuel cells (SOFC).[3] It is generally accepted that if the operating temperature of the SOFC could be reduced from the high temperatures required (typically 1000 °C) this would be a significant practical advance.[1−3] However, the conventional zirconia electrolyte does not exhibit sufficient oxygen ion conductivity to be used at lower temperatures.

Recent investigations[4−8] have discovered extremely high oxygen ion conductivity in the doped $LaGaO_3$ perovskite, which is superior to that of Y/ZrO_2 at the lower operating temperature of 800 °C. The incorporation of cation dopants (particularly Sr at La sites and Mg at Ga sites) gives rise to the highly mobile oxygen vacancies that are responsible for the observed ionic conductivity. More recent studies[7,8] have investigated the solid-solution range of the $La_{1-x}Sr_xGa_{1-y}Mg_yO_{3-\delta}$ system (LSGM) as a means of optimizing the conduction properties. It has been noted that the perovskite structure of $LaGaO_3$ also allows for a wider range in the choice of electrode materials than the fluorite-structured electrolytes. For example, the fuel cell performance of a LSGM electrolyte coupled with Pt, $LaMnO_3$, or $LaCoO_3$ cathodes has been investigated.[4]

By employing advanced computer-simulation techniques, we have previously obtained useful information on the defect and ion-transport properties of the perovskite-structured $LaMO_3$ oxides (where M = Cr, Mn, Fe, Co)[9−11] and the brownmillerite-structured $Ba_2In_2O_5$;[12] these techniques are now well-established tools in solid-state chemistry and are particularly suited to probing complex materials at the atomic level. The present study will extend this work by a detailed investigation of the $LaGaO_3$-based system, which is viewed as a promising oxygen ion conductor. Here we have focused attention on the substitution of a range of dopant ions and the formation of dopant-vacancy clusters, as well as the energetics of oxygen ion migration.

* To whom correspondence should be addressed (E-mail: m.islam@surrey.ac.uk).

Simulation Methods

The simulations are formulated within the framework of the Born model, the main features of which are the nature of the interatomic potentials and the modeling of perfect and defective lattices. The present account of these widely used techniques (embodied in the GULP code[13]) will be brief since comprehensive reviews are given elsewhere.[14]

The effective potentials describing the interatomic forces are represented by ionic, pairwise potentials of the form

$$\phi_{\alpha\beta}(r) = \frac{-Z_\alpha Z_\beta e^2}{\epsilon r} + A_{\alpha\beta}\exp(-r/\rho_{\alpha\beta}) - C_{\alpha\beta}/r^6 \qquad (1)$$

which includes a long-range Coulombic interaction and a short-range term to model the repulsions and van der Waals attractions between electron-charge clouds. Because charged defects will polarize other ions in the lattice, ionic polarizibility must be incorporated into the potential model. The shell model provides a simple description of such effects and has proven to be effective in simulating the dielectric properties of ceramic oxides.

An important feature of these calculations is the treatment of lattice relaxation about the point defect or migrating ion. The Mott−Littleton approach is to partition the crystal lattice into two regions so that ions in a spherical inner region surrounding the defect are relaxed explicitly. In contrast, the remainder of the crystal, where the defect forces are relatively weak, is treated

S1089-5647(97)02819-8 CCC: $15.00
Published on Web 03/31/1998

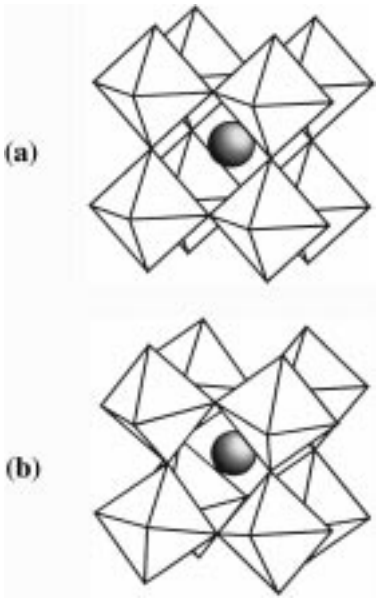

Figure 1. Perovskite crystal structure of $LaGaO_3$: (a) cubic and (b) orthorhombic.

TABLE 1: Interatomic Potentials for $LaGaO_3$

(i) Short-Range

interaction[a]	A (eV)	ρ (Å)	C (eV Å^6)
$La^{3+}\cdots O^{2-}$	1545.21	0.3590	0
$Ga^{3+}\cdots O^{2-}$	2901.12	0.2742	0
$O^{2-}\cdots O^{2-}$	22764.30	0.1490	43.0

(ii) Shell Model[b]

species	Y (e)	k (eV Å^{-2})
La^{3+}	−0.25	145.0
Ga^{3+}	3.00	99999
O^{2-}	−2.239	42.0

[a] Potential cutoff = 12 Å. [b] Y and k refer to the shell charge and harmonic spring constant, respectively.

by more approximate quasi-continuum methods. In this way, local relaxation is effectively modeled and the crystal is not considered simply as a rigid lattice through which ion species diffuse.

The potential parameters for $LaGaO_3$ were derived by empirical procedures using the observed orthorhombic perovskite structure.[15] This structure is built upon a framework of corner-linked GaO_6 octahedra; the orthorhombic phase can be considered as due purely to tilts of these octahedra from the ideal cubic configuration (shown in Figure 1). The potentials for the La−O and O−O interactions were transferred directly from the analogous simulation study of the LaMO$_3$ (where M = Cr, Mn, Fe, Co) perovskites.[9] Table 1 lists the interatomic potentials and shell model parameters used in this study. The calculated bond distances and lattice parameters and their comparison with experimental values are listed in Table 2. Examination of the differences shows good agreement between experimental and simulated structures, as well as reasonable accord with the measured dielectric constant.[16] To our knowledge these studies are the first detailed survey of the $LaGaO_3$ material employing simulation methods.

Results and Discussion

Dopant Substitution. It has been clearly shown that the addition of aliovalent dopants (especially Sr for La and Mg for Ga) is crucial to the high oxygen ion conductivity in $LaGaO_3$.[4−8]

TABLE 2: Calculated and Experimental Properties of Orthorhombic $LaGaO_3$

property	calcd	exptl
unit cell parameters		
a (Å)	5.485	5.527
b (Å)	7.752	7.781
c (Å)	5.481	5.496
$\alpha = \beta = \gamma$	90.0	90.0
bond distances (Å)		
La−O(1)	2.538	2.418
La−O(2)	2.541	2.400
Ga−O(1)	1.958	1.977
Ga−O(2)	1.960	1.956
lattice energy (eV)	−143.250	
dielectric constants		
static $\langle\epsilon_o\rangle$	16.79	∼25[a]
high frequency $\langle\epsilon_\infty\rangle$	2.02	

[a] Dube et al.[16]

Our simulation approach to dopant substitution follows that of several successful studies of impurities in oxide materials[10,17] in which the energetics of substitution are calculated. The cations are incorporated into the lattice at either La^{3+} or Ga^{3+} sites with the creation of oxygen vacancies as charge-compensating defects. Considering Sr^{2+} substitution of La^{3+} as an example, this doping process can be represented by the following defect reaction

$$SrO + La_{La}^{\times} + {}^1/_2O_O^{\times} = Sr'_{La} + {}^1/_2V_O^{\bullet\bullet} + {}^1/_2La_2O_3 \quad (2)$$

where, in Kroger−Vink notation,[18] Sr'_{La} signifies a dopant substitutional and $V_O^{\bullet\bullet}$ an oxygen vacancy. The energies of this "solution" reaction can be evaluated by combining appropriate defect and lattice energy terms. In this way such an approach provides a useful systematic guide to the relative energies for different dopant species at the same site. The resulting solution energies for a series of alkaline-earth metal and alkali metal ions in $LaGaO_3$ are presented in Figure 2 as a function of dopant radius. We note that the interatomic potentials for the dopant ions are exactly those of corresponding binary metal oxides[19] that have been applied to analogous studies of the LaMO$_3$ perovskites[9,10] and other ceramic oxides.

Examination of the results (Figure 2) reveals that the lowest and most favorable solution energies are predicted for Sr at the La site and Mg at the Ga site. The favorable incorporation of these two ions will therefore enhance oxygen diffusivity owing to the increase in the concentration of oxygen vacancies. These results agree well with experimental work[4−8] in which Sr and Mg are the favored acceptor dopants used to produce high oxygen ion conductivity. It is also apparent from Figure 2 that a degree of correlation is found between the calculated solution energy and the dopant size with minima near the radii of the host cations. We note that the solution energies for the alkali metal dopants in $LaGaO_3$ are appreciably endothermic, in line with their observed low solubility.

As a possible predictive tool, this approach was then extended to a wider range of low-valent ions substituting at both La and Ga sites; the calculated solution energies are presented in Figure 3, which includes the Sr and Mg ions as reference points. Examination of the results confirms that Sr is the most favorable dopant on the La site. In contrast, we find that Cu^{2+} and Hg^{2+} have lower solution energies than Mg^{2+} on the Ga sublattice. This predicts that both Cu and Hg ions are potential candidates for use as acceptor dopants in $LaGaO_3$ to enhance the oxygen diffusivity. It is worth noting that a related system, $LaSrCuGaO_5$, has been synthesized and adopts the brownmillerite

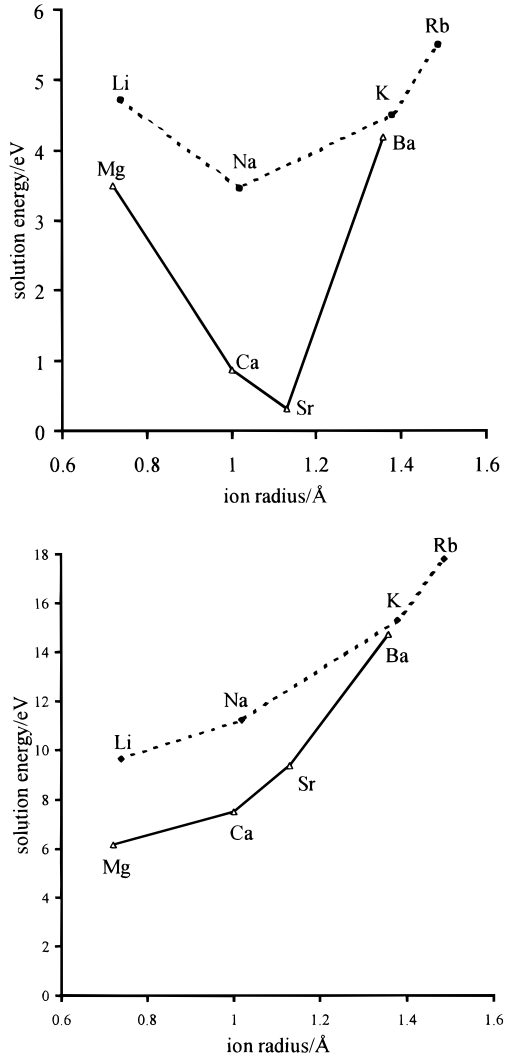

Figure 2. Calculated energies of solution as a function of dopant radius for alkali and alkaline-earth cations: (a) La site and (b) Ga site.

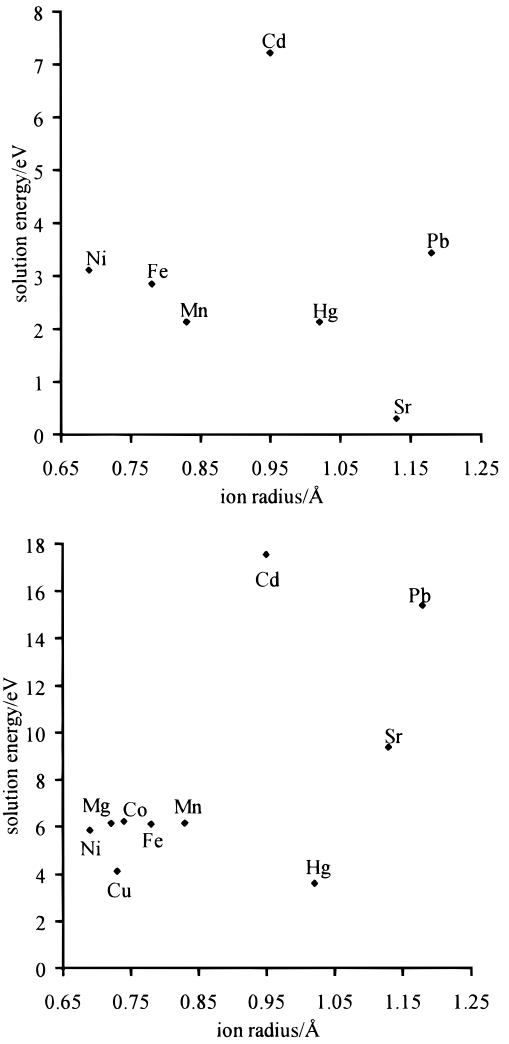

Figure 3. Calculated energies of solution as a function of dopant radius: (a) La site and (b) Ga site.

structure.[20] While we recognize the possible electronic contribution from mixed-valence copper, these results suggest that Cu- or Hg-doped $La_{1-x}Sr_xGaO_{3-\delta}$ warrants further experimental investigation. In this respect, it is interesting to note that one of the highest oxygen ion conductivities is observed in the Aurivillius phase Cu-doped $Bi_4V_2O_{11}$ ("BICUVOX"). Transport number measurements indicate that the oxygen ions are the predominant charge carriers in this material with a very small electronic contribution related to the vanadium ions.[21]

Dopant−Vacancy Clusters. It is well-known that interactions between dopant ions and their charge-compensating defects can lead to the formation of distinct clusters which can "trap" the migrating species. For example, the ionic conductivity of fluorite-structured oxides (such as Y-doped CeO_2) is largely controlled by the extent of dopant−vacancy interactions.[1,4,22] These have been described in terms of the formation of dopant−oxygen vacancy pair clusters for low dopant concentrations, which add a binding energy term (E_{bind}) to the conduction activation energy.

From ionic conductivity measurements of $La_{1-x}Sr_xGa_{1-y}Mg_yO_{3-\delta}$, Huang and Petric[7] find significant differences in the activation energy as a function of the Sr and Mg content. Drennan et al.[8] also observe a large difference in the conduction activation energy between data at low temperature (E_{act} = 109 kJ mol^{-1}) and at high temperature (E_{act} = 64 kJ mol^{-1}). Feng and Goodenough[6] have noted the importance of the possible trapping of an oxygen vacancy at a divalent-cation impurity. Consequently, we undertook a series of calculations on defect pair clusters in the $LaGaO_3$ system comprised of a dopant substitutional and an oxygen vacancy at nearest-neighbor sites. Since Sr on La and Mg on Ga are the most commonly used acceptor dopants, and Cu and Hg are also calculated to be favorable, we have focused our attention on these substitutionals. X-ray diffraction data[7] of $La_{1-x}Sr_xGa_{1-y}Mg_yO_{3-\delta}$ indicate a transition from an orthorhombic to cubic structure at higher dopant levels corresponding to $x + y = 0.35$. We have therefore considered cluster formation in both the orthorhombic and cubic phases of $LaGaO_3$, with calculated cluster binding energies with respect to the component isolated defects reported in Table 3.

TABLE 3: Calculated Binding Energies for Dopant−Oxygen Vacancy Pair Clusters in Cubic and Orthorhombic $LaGaO_3$

		E_{bind} (eV)[b]	
dopant site	cluster[a]	cubic	orthorhombic
Sr on La	$(Sr'_{La}V^{\bullet\bullet}_O)$	−0.02	−0.37
Mg on Ga	$(Mg'_{Ga}V^{\bullet\bullet}_O)$	−1.83	−1.77
Cu on Ga	$(Cu'_{Ga}V^{\bullet\bullet}_O)$	−1.34	−1.50
Hg on Ga	$(Hg'_{Ga}V^{\bullet\bullet}_O)$	−1.76	−1.90

[a] Oxygen vacancy is at a nearest-neighbor site. [b] Sign convention: negative value indicates system is bound.

TABLE 4: Calculated and Experimental Energies for Oxygen Ion and Cation Vacancy Migration in $LaGaO_3$

ion	E_{mig}^{calc} (eV)	E_{act}^{exp} (eV)
O^{2-}	0.73	0.79,[a] 1.07,[b] 0.81−1.17,[c] 0.66,[d] 1.13[d]
La^{3+}	4.66	
Ga^{3+}	16.92	

[a] Ishihara et al.[5] [b] Feng and Goodenough.[6] [c] Huang and Petric.[7] [d] Drennan et al.[8]

The results reveal that all the pair clusters are bound with the lowest binding energy for the Sr−vacancy configuration. In particular, we find a near-zero value for $(Sr'_{La}V_O^{\bullet\bullet})$ in the cubic structure although it is possible that other types of aggregates could have greater stability. This suggests a negligible change in conduction activation energy with Sr level for compositions with cubic symmetry. Any change in activation energy with increasing Sr dopant concentration may be linked to the changes in the overall crystal structure. In any case, these findings suggest that the oxygen vacancies originating from Sr doping will optimize the ionic conductivity to a greater degree owing to the minimum binding energy term. By contrast, we find that Mg−vacancy clusters have much higher binding energies; this points to strong "trapping" of the migrating oxygen vacancies with increasing Mg concentration. This result is consistent with the observed increase in the conduction activation energy and decrease in conductivity at higher Mg doping levels in $La_{0.8}Sr_{0.2}Ga_{1-y}Mg_yO_{3-\delta}$.[7]

We should note that it is has been observed that Mg doping is important in promoting the introduction of a higher concentration of Sr into $LaGaO_3$. This indicates a synergy effect when doping simultaneously both A (La) and B (Ga) lattice sites, so that the solubility limit for each dopant increases relative to the singly doped material.

While our calculations also find high cluster binding energies for both Cu and Hg ions, the magnitude for Cu is less than for the commonly used Mg dopant. Previous work on dopants in fluorite oxides have indicated that the elastic strain field around the defects in the cluster is at least as important as the electrostatic interaction.[22] The binding energy is therefore dependent upon the ion size "mismatch" between the host and dopant cation with the expectation of a minimum when the ionic radii are approximately the same. This is borne out here with the greater ion size mismatch for the Mg^{2+} (0.72 Å) on the small Ga^{3+} site (0.62 Å).

Perhaps the most significant conclusion from the cluster calculations is that Mg has a much stronger tendency to "trap" the migrating oxygen vacancy than the Sr dopant. Incorporation of Sr into $LaGaO_3$ will optimize the ionic conductivity owing to both the low binding energy term and the increase in vacancy concentration.

Anion and Cation Migration. Despite the conductivity studies on $LaGaO_3$ referred to above, fundamental mechanistic features of oxygen transport are not well-characterized. Calculations can greatly enhance our understanding of this problem by probing the energetics of oxygen vacancy migration, which effects the transport of lattice O^{2-}. It is worth recalling that the simulation approach is able to model lattice relaxation about the migrating ion and treats ionic polarizability by the shell model. In this way, the $LaGaO_3$ structure is not considered simply as a hard-sphere lattice with fixed ions.

The saddle-point configuration to vacancy migration in the cubic structure has been identified from which the energy barrier was derived. In Table 4 we report the calculated migration energies (E_{mig}) together with available activation energies (E_{act}) from experimental studies. Our calculated migration energy (0.73 eV) for oxygen transport accords well with activation energies of 0.79 and 0.66 eV from SIMS measurements of oxygen self-diffusion[5] and dc conductivity studies over a high temperature range (850−1000 °C),[8] respectively. However, we recognize that direct comparison is not straightforward since the observed values show significant scatter. Such variation may reflect differences in synthesis conditions and doping levels, as well as problems associated with deviations from ideal stoichiometry.

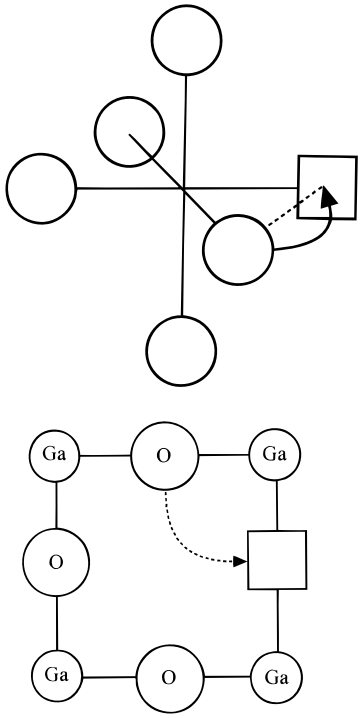

Figure 4. Schematic representation of the curved path for oxygen vacancy migration: (a) GaO_6 octahedron and (b) [Ga−O] *ab*-plane.

It is important to stress that E_{mig} relates purely to migration of the oxygen vacancy and does not include a binding (or association) term. Examination of Table 4 also reveals that some experimental studies find higher activation energies of ca. 1.1 eV. As earlier studies of fluorite oxides have already shown,[3,22] the formation of $(M'_AV_O^{\bullet\bullet})$ pair clusters adds a term equal to half the binding energy (E_{bind}) to the Arrhenius energy of the conductivity. Our strong binding energy term for the $(M'_{Ga}V_O^{\bullet\bullet})$ cluster may help to rationalize the increase in E_{act} with increasing Mg content in LSGM. In general, the increase in activation energy at higher doping levels may be attributed to the onset of significant defect clustering.

Analysis of the calculated migration mechanism along the ⟨110⟩ edge of the GaO_6 octahedron reveals that the pathway is not strictly linear. Rather, the simulations suggest a curved route with the saddle point slightly bowed away from the neighboring Ga ion (shown in Figure 4), which results in a significantly lower oxygen migration energy.

In the saddle-point configuration, the migrating oxygen ion must pass through the opening of a triangle defined by two La^{3+} ions and one Ga^{3+} ion (Figure 5). We find significant outward relaxation (∼0.1 Å) of these cations away from the mobile oxygen ion, which probably reduces any repulsive overlap interactions. Our earlier work on ABO_3 shows a strong relationship between the perovskite tolerance factor (t) and the

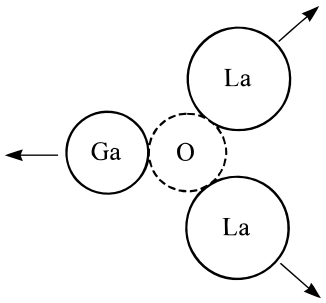

Figure 5. Saddle-point configuration of oxygen ion migration indicating cation relaxation.

migration energy, in which the minimum seems to correspond to the most effective balance of the relaxation of A and B cations.[9]

Despite numerous studies devoted to oxygen transport, little attention has been paid to cation diffusion in $LaGaO_3$, notwithstanding its significance to the reliability of technological applications. Knowledge of cation diffusion is central to high-temperature processes such as sintering, creep, and grain growth, as well as to interactions at the electrolyte−electrode interface. The existence of cation vacancies may become particularly important in $LaGaO_3$ samples that deviate from ideal cation stoichiometry, as is observed in similar perovskite oxides.[23] In a preliminary attempt to shed light on this problem, we have undertaken atomistic simulations of vacancy migration on the La and Ga lattices. Possible vacancy jumps between neighboring cation sites have been identified with resulting migration energies included in Table 4.

As was expected, the calculations reveal high migration energies for cation vacancy transport, which confirms the much slower diffusion rates in comparison to oxygen. Analysis of the crystal structure indicates that the jump distance for La motion (3.87 Å) is shorter than that for Ga motion (5.48 Å), and that the saddle point for a migrating Ga ion is very close to two La lattice ions. While there is no experimental data for direct comparison, the magnitude of the calculated values is consistent with observed activation energies of >4eV for cation diffusion in other perovskite-type oxides.[24] In view of the high migration energy for Ga, we anticipate the diffusion coefficients following the order $D_O \gg D_{La} > D_{Ga}$. The diffusion of Ga is therefore likely to be rate-controlling for processes such as creep or grain growth. Further detailed studies of ion diffusion are currently underway using molecular dynamics (MD) techniques.

Holes and Protons in Doped Oxide. It has been reported that doped $LaGaO_3$ shows a small amount of hole conductivity at high oxygen partial pressures.[4] However, recent studies suggest this is not the case by comparison of the oxygen self-diffusivity obtained from tracer and ionic conductivity.[5] We have therefore examined the energetics of hole formation in $LaGaO_3$ via the following oxidation reaction

$$V_O^{\bullet\bullet} + {}^1/_2O_{2(g)} = O_O^{\times} + 2h^{\bullet} \qquad (3)$$

which involves the "filling" of oxygen vacancies to create holes ($h^{\bullet}$). Our approach to electronic defects follows that used for $LaMO_3$ and $Ba_2In_2O_5$[10,12] in which we model the hole center as Ga^{4+} or O^-. The resulting energies, listed in Table 5, favor creation of oxygen holes. This is not too surprising since it is known that the group 13/III elements have a maximum oxidation state of +III.

Using the oxygen hole term, the energy for the oxidation reaction (3) can be evaluated and is found to be 3.78 eV (Table 5). This result suggests a highly unfavorable process, indicating that ionic rather than electronic compensation (and hence ionic rather than p-type conductivity) predominates in doped $LaGaO_3$, which is in agreement with recent tracer experiments.[5] Such redox behavior is in contrast to that found in the perovskite oxides containing transition-metal ions at the B-site (e.g., $LaCoO_3$) but is similar to the properties of $LaAlO_3$.[10] It has been reported that an advantage of acceptor-doped $LaGaO_3$ over similar CeO_2-based electrolytes is that it is stable in both oxidizing and reducing atmospheres.[4] In general, our calculations are consistent with experimental findings that show that the $LaGaO_3$ system is mainly an ionic conductor with an ionic transport number close to unity.[5,8]

TABLE 5: Calculated Energies of Hole Formation

defect process[a]	energy (eV)
Ga^{4+} ($h^{\bullet}$)	19.52
O^- ($h^{\bullet}$)	7.88
$V_O^{\bullet\bullet} + {}^1/_2O_{2(g)} = O^x_O + 2h^{\bullet}$	3.78

[a] Ionization energy (Ga IV 64 eV); electron affinity (O II 8.75 eV).

TABLE 6: Terms Used in the Calculation of the Energy of Water Incorporation (E_{H_2O})

term	energy (eV)	term	energy (eV)
E_{OH}	17.24[a]	E_{PT}	−11.77
E_{V_O}	19.62	E_{H_2O}	3.10

[a] Includes D of Morse potential.[11]

In addition to hole formation, there is also the question of whether there is any evidence of protons in this material. Perovskite-structured oxides, particularly $BaCeO_3$ and $SrCeO_3$, have already received considerable attention as high-temperature proton conductors.[25,26] Protons are introduced into these doped materials by treatment in water vapor, whereby oxygen vacancies are filled by hydroxyl ions. The defect is described as a hydroxyl group as the interstitial proton is clearly associated with the neighboring oxygen ion. The water incorporation reaction can be described as follows:

$$H_2O + V_O^{\bullet\bullet} + O_O^{\times} = 2OH_O^{\bullet} \qquad (4)$$

We have investigated this problem by evaluating the energy for this incorporation reaction (E_{H_2O}) by using the following reaction

$$E_{H_2O} = 2E_{OH} - E_{V_O} + E_{PT} \qquad (5)$$

where E_{OH} is the energy associated with substitution by the hydroxyl group, E_{V_O} the energy of an oxygen vacancy, and E_{PT} the energy of the proton-transfer reaction: $O^{2-} + H_2O \rightarrow 2OH^-$. These component energy terms and the calculated value of E_{H_2O} are given in Table 6. As in our previous simulation studies of protons in perovskite oxides, the O−H interaction is modeled as a Morse potential.[11] There are, of course, uncertainties in the absolute values owing to the free-ion energies employed. However, the endothermic energy for E_{H_2O} suggests that the dissolution of protons at the expense of oxygen vacancies is highly unfavorable. We note that our previous calculations find E_{H_2O} to be exothermic for both $LaMnO_3$ and $SrTiO_3$, which are compatible with observation.[11] Although quantitative data for doped $LaGaO_3$ is limited, our result is consistent with the work of Feng and Goodenough[6] who found no evidence of proton conduction in LSGM by examining the conductivity in three different air atmospheres: dry, ambient, and water-saturated.

Conclusion

The present study illustrates how atomistic modeling techniques can contribute to the understanding of key aspects of $LaGaO_3$ that are relevant to its potential use in fuel cells and other similar applications. The following points have emerged from our results:

(1) Favorable acceptor dopants (on energetic grounds) are Sr^{2+} at La and Mg^{2+} at Ga; these results accord well with experimental work that finds the highest ionic conductivity in the (La, Sr)(Ga, Mg)$O_{3-\delta}$ system. The favorable "solution" of these dopants will enhance oxygen diffusivity owing to the increase in the oxygen vacancy concentration. We also suggest that Cu^{2+} and Hg^{2+} warrant further investigation as potential candidates as acceptor dopants (at the Ga site).

(2) The binding energies for defect clusters indicate that the Mg^{2+} substitutional has a strong tendency to "trap" the migrating oxygen vacancy. This result is compatible with the observed increase in activation energy and decrease in conductivity at higher Mg doping levels in $La_{0.8}Sr_{0.2}Ga_{1-y}Mg_yO_{3-\delta}$. However, Sr doping will enhance oxygen ion conductivity to a greater degree owing to the minimum binding energy term.

(3) Our calculated migration energy (0.73 eV) for oxygen vacancy transport is generally consistent with measured values. Higher activation energies may be related to dopant−vacancy association at higher dopant concentrations. The mechanism for oxygen vacancy migration is along the GaO_6 octahedron edge, but following a slightly curved trajectory with significant outward relaxation of adjacent cations.

(4) The first reported examination of cation transport in $LaGaO_3$ reveals high vacancy migration energies (>4 eV) and confirms the much slower diffusion rates in comparison to oxygen. The diffusion of Ga^{3+} is likely to be rate-controlling for processes such as creep or grain growth.

(5) Oxidation with the formation of holes is an energetically unfavorable process. This is consistent with experimental findings that show doped $LaGaO_3$ to be almost a pure ionic conductor. Preliminary calculations find that the incorporation of water is appreciably endothermic, which suggests that proton conduction will not be significant in this material.

Acknowledgment. We thank J. D. Gale, A. Dicks, and J. A. Kilner for valuable discussions. This work was financially supported by BG plc (Gas Research and Technology Centre). The simulations were carried out on the computing facilities at the Rutherford Appleton Laboratory.

References and Notes

(1) Steele, B. C. H. In *Solid State Ionics*; Balkanski, Takahashi, Tuller, H. L., Eds.; Elsevier: Amsterdam, 1992; *Solid State Ionics* **1996**, *86*−*88*, 1223.

(2) Kendall, K. R.; Navas, C.; Thomas, J. K.; zur Loye, H. C. *Solid State Ionics* **1995**, *82*, 215.

(3) Minh, N. Q. *J. Am. Ceram. Soc.* **1993**, *76*, 563. Tuller, H. L. *J. Phys. Chem. Solids.* **1994**, *55*, 1393.

(4) Ishihara, T.; Matsuda, H.; Takita, Y. *J. Am. Chem. Soc.* **1994**, *116*, 3801; *Solid State Ionics* **1995**, *79*, 147. Ishihara, T.; Minami, H.; Matsuda, H.; Nishiguchi, H.; Takita, Y. *Chem. Commun.* **1996**, 929.

(5) Ishihara, T.; Kilner, J. A.; Honda, M.; Takita, T. *J. Am. Chem. Soc.* **1997**, *119*, 2747.

(6) Feng, M.; Goodenough, J. B. *Eur. J. Solid State Inorg. Chem.* **1994**, *31*, 663.

(7) Huang, P.; Petric, A. *J. Electrochem. Soc.* **1996**, *143*, 1644.

(8) Drennan, J.; Zelizko, V.; Hay, D.; Ciacchi, F. T.; Rajendran, S.; Badwal, S. P. S. *J. Mater. Chem.* **1997**, *7*, 79.

(9) Cherry, M.; Islam, M. S.; Catlow, C. R. A. *J. Solid State Chem.* **1995**, *118*, 125; Islam, M. S.; Cherry, M.; Catlow, C. R. A. *J. Solid State Chem.* **1996**, *124*, 230.

(10) Islam, M. S.; Cherry, M.; Winch, L. J. *J. Chem. Soc., Faraday Trans.* **1996**, *92*, 479.

(11) Islam, M. S.; Cherry, M. *Solid State Ionics* **1997**, *97*, 33. Cherry, M.; Islam, M. S.; Gale, J. D.; Catlow, C. R. A. *J. Phys. Chem.* **1995**, *99*, 14614.

(12) Fisher, C. A. J.; Islam, M. S.; Brook, R. J. *J. Solid State Chem.* **1997**, *128*, 137.

(13) Gale, J. D. *J. Chem. Soc., Faraday Trans.* **1997**, *93*, 629.

(14) Catlow, C. R. A. In *Solid State Chemistry: Techniques*; Cheetham, A. K., Day, P., Eds.; Clarendon Press: Oxford, 1987.

(15) Wang, Y.; Liu, X.; Yao, G.-D.; Liebermann, R. C.; Dudley, M. *Mater. Sci. Eng. A* **1991**, *132*, 13.

(16) Dube, D. C.; Scheel, H. J.; Reaney, I.; Daglish, M.; Setter, N. *J. Appl. Phys.* **1994**, *75*, 4126.

(17) Donnerberg, H.; Tomlinson, S. M.; Catlow, C. R. A.; Schirmer, O. F. *Phys. Rev. B* **1991**, *44*, 4877. Grimes, R. W. *J. Am. Ceram. Soc.* **1994**, *77*, 378.

(18) Kroger, F. A. in *The Chemistry of Imperfect Crystals*; North-Holland:Amsterdam, 1974.

(19) Lewis, G. V.; Catlow, C. R. A. *J. Phys. C* **1985**, *18*, 1149.

(20) Kharlanov, A. L.; Antipov, E. V.; Bryntse, I.; Luzikova, A. V.; Kouba, L. M. *Eur. J. Solid State Inorg. Chem.* **1992**, *29*, 1041.

(21) Mairesse, G. In *Fast Ion Transport in Solids*; Scrosati, B., Ed.; Kluwer Academic: Amsterdam, 1993.

(22) Kilner, J. A.; Brook, R. J. *Solid State Ionics* **1982**, *6*, 237.

(23) Van Roosmalen, J. A. M.; Cordfunke, E. H. P.; Helmholdt, R. B. *J. Solid State Chem.* **1994**, *110*, 100.

(24) Chen, N.; Rothman, S. J.; Routbort, J. L. *J. Mater. Res.* **1992**, *7*, 2308.

(25) Iwahara, H. *Solid State Ionics* **1995**, *77*, 289.

(26) Kreuer, K. D. *Chem Mater.* **1996**, *8*, 610.